Journal of Microscopy , Vol. 238, Pt 3 2010, pp. 218–229
Received 26 June 2009; accepted 21 September 2009
doi: 10.1111/j.1365-2818.2009.03343.x

Automatic twin statistics from electron backscattered diffraction data

P.E. MARSHALL*, G. PROUST†,‡, J.T. ROGERS§ & R.J. MCCABE*
*Materials Science and Technology Division, Los Alamos National Laboratory, Los Alamos, New Mexico 87545, U.S.A.
†School of Civil Engineering, University of Sydney, Sydney, NSW 2006, Australia
‡Australian Key Centre for Microscopy and Microanalysis, University of Sydney, Sydney, NSW 2006, Australia
§Materials Department, University of California, Santa Barbara, California 93106, U.S.A.

Key words. EBSD, magnesium, twinning, uranium, zirconium.

Summary

A new computer code has been developed to automatically extract quantitative twin statistics from electron backscatter diffraction data. The new code is an improvement upon previous codes in that it handles materials of any crystal symmetry, type I, Type II and compound twins, and general stress states. Moreover, accuracy of the results has been greatly improved. In addition, twin statistics including number, area fraction, twin thickness and twinning dependencies on orientation, grain size and neighbourhood effects can be routinely analysed. The new code has been applied to scan data from deformed magnesium, zirconium and uranium, and can potentially be used for any twinning material for which reliable electron backscatter diffraction results can be obtained.

Introduction

Twinning is an important deformation mode in hexagonal close-packed metals such as zirconium (Bingert *et al.*, 2002; McCabe *et al.*, 2006, 2009), titanium (Salem *et al.*, 2002) and magnesium (Wagoner *et al.*, 2007; Brown *et al.*, 2009), and metals of less symmetric crystal structures such as uranium (Brown *et al.*, 2009). To better predict and model the mechanical behaviour and texture evolution of these materials, it is essential to account for the effects of twinning. Some crystal plasticity models contain schemes that allow crystallographic reorientation by twinning (Van Houtte, 1978; Tome *et al.*, 1991; Kalidindi, 1998; Wu *et al.*, 2007) to accurately predict texture evolution. A more recently developed scheme, the composite grain twin model (Proust *et al.*, 2007), also accounts for the hardening induced by the creation of twins within grains. To ensure that these models accurately predict the effects of twinning on mechanical properties and microstructural evolution, quantitative experiments measuring twinning statistics are required. Obtaining such information has been difficult, especially in metals that exhibit multiple twinning modes and multiple generations of twins (twins within twins) (McCabe *et al.*, 2009).

Electron backscatter diffraction (EBSD) is a technique that has been useful in the study of twins (Bingert *et al.*, 2002; Glavicic *et al.*, 2004; Battaini *et al.*, 2007; McCabe *et al.*, 2009). EBSD is a scanning electron microscopy technique where the electron beam is scanned across the sample and an EBSD pattern is indexed to determine the crystal orientation at each scan point on a pre-defined grid. The advantages and disadvantages of EBSD twin analysis as compared to optical microscopy, TEM and neutron diffraction have been previously discussed in some detail (Henrie *et al.*, 2004, 2005; McCabe *et al.*, 2009). In brief, EBSD offers a unique combination of spatially correlated orientation data and a large sampling area appropriate for statistical twin analysis. The spatially resolved orientation data inherent to EBSD lends itself well to automatic twin identification and analysis.

There have been a number of previous attempts to measure twin statistics using EBSD data, all successful to varying degrees and all based upon the same key ideas. In order to use EBSD data for twin statistics analysis one needs to: (1) accurately determine which boundaries are twin boundaries and of which type and (2) determine which of two orientations sharing this twin relationship is the pre-twinning orientation (parent) and which is the twin (child). Mason *et al.* (2002) proposed a three criteria scheme for defining twin boundaries involving misorientation, K_1 matching and alignment of the trace of the twin composition plane with the trace of

Correspondence to: Rodney J. McCabe. Tel: +1-505-606-1649; fax: +1-505-667-8021; e-mail: rmccabe@lanl.gov

a K_1 plane. The twin composition plane is the plane that physically separates the twinned region from the parent and is orthogonal to the thickening direction. It is equivalent to the K_1 plane for a coherent twin. They also suggested that some consideration of Schmid factor and twin morphology could be used to distinguish parent from child. Wright *et al.* (2002) later implemented a scheme to distinguish parent from child based on a majority rule, where the parent orientation is the orientation with the largest number of scan points in a grain. Henrie *et al.* (2004) developed a more accurate, semi-automated scheme in which the identification of the parent was determined manually and then a computer code identified the different twin modes and generations within a grain. Henrie *et al.* (2005) improved this technique by eliminating the manual input and automatically selecting the parent within a grain following a voting scheme based on majority rule, aspect ratio, Schmid factor and consideration of the total number of twin generations.

Compared to previous EBSD codes, the code based on the present work has broadened applicability, increased utility and improved accuracy. Although the starting point for our development was the code of Henrie *et al.* (2005), the new code is considerably different in many aspects and has three significant changes. First, the code has been extended to handle materials of any crystal symmetry (there are some limitations for cubic materials that will be discussed later). Second, compound, type I and type II twins can all be analysed, and effective Schmid factors can be computed for any stress state. Finally, more effective use of twin morphology and neighbour analysis is incorporated for determining parent/child relationships and dealing with twin relationship anomalies. The code has been tested on experimental data from the hexagonal close-packed metals Zr and Mg and on the orthorhombic metal U.

Experimental

Much of the experimental detail is given elsewhere, especially with regard to the processing, mechanical testing and preparation of the Zr (McCabe *et al.*, 2009), Mg (Livescu *et al.*, 2006) and U (Brown *et al.*, 2009) used in this study. We have however changed the sample preparation for Mg, to get more reliable EBSD data, to mechanical polishing to 1 μm diamond followed by immersion for 15–30 s in 10% nitric acid and water. We used a TSL system for our EBSD data collection and TSL OIM^{TM} Analysis software for our EBSD data analysis. The EBSD data was collected in an FEI XL30 microscope at 20–25 kV in a hexagonal grid with a step size of 0.2 μm for Zr and U and a step size of 0.5 μm for Mg.

Twin code

Prior to giving a description of how the program works, a few terms used throughout this paper to describe different regions of an EBSD scan are defined. The fundamental unit of the EBSD scan is the scan point. Associated with each scan point is a crystallographic orientation with respect to the sample axes defined by a set of three Euler angles (φ_1, Φ, φ_2), an (x, y) position, a phase, and several other EBSD parameters not utilized in this work. A set of neighbouring scan points sharing the same orientation, within some user-defined threshold (generally 5°), is defined as a grain fragment. A whole grain is defined as a group of fragments all sharing at least one twin relationship with a neighbouring fragment. Within individual whole grains, families are defined as groups of grain fragments having the same average orientation within some user-defined threshold (generally 15°). These families may be fragments of the parent orientation that are separated by twins or different lamellae of the same twinning variant. Ultimately, all families will be classified as either parent phase, a phase corresponding to a specific twinning mode and generation (first generation twins form inside the parent, second generation twins form inside first generation twins, etc.), or a phase defined as other. Figure 1 illustrates how the families are indentified in a grain: Fig. 1(a) shows an orientation map of a whole grain and Fig. 1(b) shows how the different grain fragments are grouped into families of similar orientations. The twin boundaries are highlighted to show the different twin relations present in this particular grain.

As mentioned previously, in order to use EBSD data for statistical twin analysis one needs to accurately determine which boundaries are twin boundaries (and of which type), and determine which of two grain fragments (or families) sharing a twin relationship is the parent and which is the child. In general this is done by first having the OIM^{TM} Analysis software group neighbouring scan points into fragments and grain fragments into whole grains. These data are then read into our twin program which groups fragments within whole grains into families, makes parent/child determinations for families sharing twin relationships, determines the phase (twin mode and generation) and twin variant for each family based on all of the parent/child determinations for the whole grain, and then calculates other twin statistics. Various output files are then generated including an OIM^{TM} Analysis readable file used for visualization, where each twin mode and generation is defined as a phase, and several text files containing twin statistics.

Coordinate systems, twin boundaries, misorientation, K_1 matching and equivalent Schmid factor

It is constructive to consider several frames of reference when analysing potential twin boundaries. The first two are the sample coordinate system, C_s, and crystal coordinate system, C_c. For details on these and their relationships see references (Kocks *et al.*, 1998; Randle & Engler, 2000). Briefly, C_s defines the orientation of the bulk sample, with the principle axes often associated with the form, shape, processing, or loading directions of the sample (i.e. the rolling direction, transverse

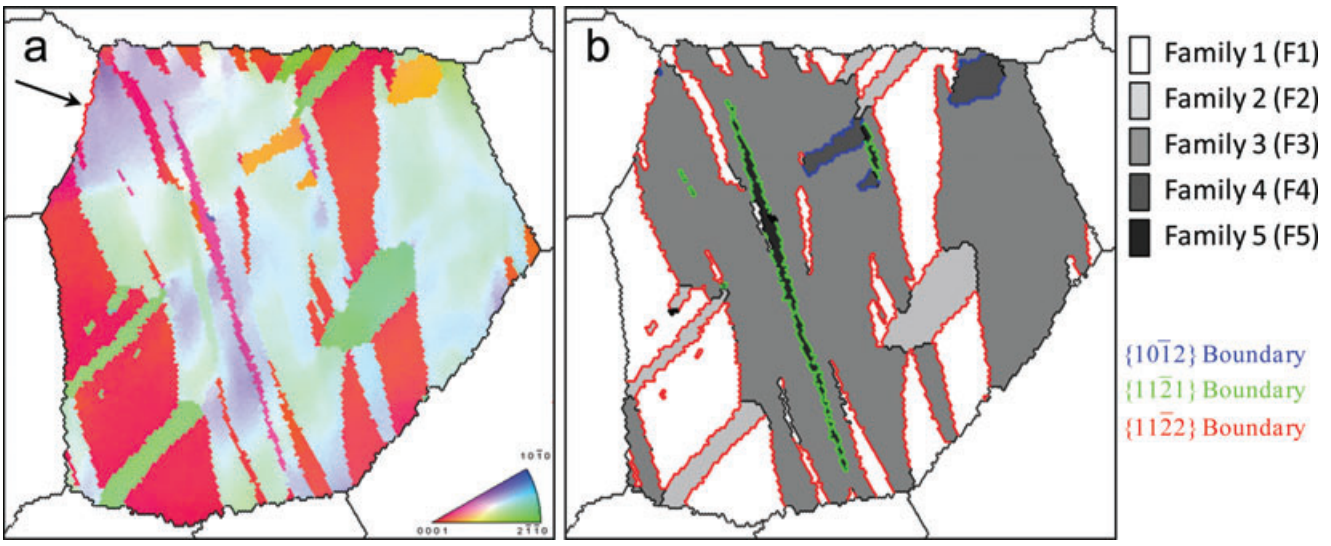

Fig. 1. (a) TT direction orientation map of a single whole grain in Zr compressed at 76 K in the TT direction to 6% strain. (b) Map of the same region showing the five different families within the whole grain and the different twin boundaries as determined based on misorientation. Note there is an erroneous twin boundary indicated by an arrow between one of the family 3 fragments and the neighbouring whole grain in the upper left of the figure requiring the other whole grain to be split off.

direction and normal direction of a rolled plate). For C_c we use an orthonormal representation of crystal directions (Young & Lytton, 1972). The orientation of C_c is related to C_s through the relationship

$$C_c = gC_s \tag{1}$$

where g is a 3×3 orientation matrix and its elements are the direction cosines between the principle axes of C_s and C_c. However, crystal lattice structures possess a number of symmetry elements, L_i, resulting in the same number of equivalent orientations. For example, there are 12 symmetry elements for the hexagonal materials belonging to Laue group 622 resulting in 12 equivalent orientation matrices.

A third useful frame of reference for analysing twins is the twin frame of reference, C_t (Kocks *et al.*, 1998). The principle axes of the twin frame of reference are the twin shear direction, the normal to the plane of shear, and the normal to the twin plane. In the crystal coordinate system these are η_1, S and K_1. The plane of shear is the plane perpendicular to K_1 that contains η_1, thus its normal (S) is perpendicular to K_1 and η_1. The twin coordinate system is related to the crystal coordinate system through the relationship $C_t = R^{\mathrm{tw}}C_c$, where

$$R_{\mathrm{tw}} = \begin{pmatrix} \eta_1 \\ S \\ K_1 \end{pmatrix}. \tag{2}$$

Two fragments sharing a twin relationship are misoriented relative to one another by 180° about the K_1 normal for a type I twin, 180° about the η_1 direction for a type II twin, or 180° about either the K_1 normal or the η_1 direction for a compound twin. These are represented in the twin reference frame by the twinning transformation matrices

$$t^{\mathrm{I}} = \begin{pmatrix} -1 & 0 & 0 \\ 0 & -1 & 0 \\ 0 & 0 & 1 \end{pmatrix} \quad t^{\mathrm{II}} = \begin{pmatrix} 1 & 0 & 0 \\ 0 & -1 & 0 \\ 0 & 0 & -1 \end{pmatrix}. \tag{3}$$

Considering the three reference frames and the twinning transformation,

$$R_{\mathrm{tw}}g_b = tR_{\mathrm{tw}}g_a \tag{4}$$

relates the orientations of two fragments sharing a twin relationship, where g_a and g_b are the orientation matrices for fragment a and fragment b, respectively. Equation 4 is essentially the criterion we use, with a tolerance angle, to determine whether two fragments share a twin relationship. A little mathematical manipulation results in the equivalent criterion $g_b g_a^T = R_{\mathrm{tw}}^T t R_{\mathrm{tw}}$. Considering all of the symmetry operations for g_b and g_a, our criterion for two fragments sharing a twin boundary becomes

$$L_1 g_b g_a^T L_J^T = R_{\mathrm{tw}}^T t R_{\mathrm{tw}} \tag{5}$$

In this equation $L_i g_b g_a^T L_j^T$ is the misorientation, M_{ab}, between fragments a and b and $R_{\mathrm{tw}}^T t R_{\mathrm{tw}}$ is the twin misorientation, M_t. To implement the 5° tolerance we measure whether the misorientation between M_{ab} and M_t is less than 5° for all combinations of L_i and L_j for the crystal system. This approach automatically considers all twin variants for a twin mode.

Once a twinning relationship is found, it is straightforward to calculate the resolved shear stress on the twin system in both fragments sharing the twin relationship. The resolved shear stress on the twin system is the shear stress acting on the K_1 plane in the η_1 direction, σ_{13}^t, in the twin coordinate system. If we have a general stress state in the specimen coordinate

system, σ^S_{kl}, then the resolved shear stress in one fragment is given by $\sigma^a_{13} = a^a_{1k}a^a_{3l}\sigma^S_{kl}$ and the resolved shear stress in the other fragment is given by $\sigma^b_{13} = a^b_{1k}a^b_{3l}\sigma^S_{kl}$, with $a^a = R^{tw}L_a g_a$ and $a^b = R^{tw}L_b g_b$, where L_a and L_b are the symmetry operators for which the two fragments share the twinning relationship. As either K_1 or η_1 are in opposite directions for the two fragments sharing a twin relationship, the resolved shear stress in the two will have approximately the same magnitude, but opposite signs. We also define the effective Schmid factor as $\sigma^t_{13}/2\tau_{max}$, where τ_{max} is the maximum shear stress for the loading conditions. The maximum shear stress is determined by converting the general specimen stress state into principal stress components and taking half of the difference between the maximum and minimum principal stress components, $\tau_{max} = (\sigma_1 - \sigma_3)/2$ (Courtney, 1990). The effective Schmid factor has a maximum of 0.5 a minimum of –0.5 and is equivalent to the Schmid factor calculated as the product of the cosines between the stress direction and the twin plane and directions, respectively, for uniaxial stress states. The effective Schmid factor will be referred to as the Schmid factor through the remainder of this article.

Interestingly, it is not possible to uniquely determine the twin variant and thus Schmid factor for fcc crystals and it is difficult for body-centered cubic (bcc) crystals. This is most obvious when considering the three face-centered cubic (fcc) twin variants $(111)[11\bar{2}]$, $(111)[1\bar{2}1]$ and $(111)[\bar{2}11]$. There is no way to distinguish between these three variants using misorientation, K_1 matching, or K_1 trace/composition plane trace analysis (the misorientations for each of these variants are identical, 180° rotation about (111), and the K_1 planes are identical. The dilemma with the bcc twin system $\{112\} < 111 >$ is similar in that measures of crystallographic misorientation alone cannot be used to uniquely define the twin variant. However, because each twin variant has a unique $\{112\}$ twin plane, the variant can be determined if the K_1 plane can be correlated with a twin composition plane. Because of these limitations, Schmid factor cannot be used to make twin determinations in cubic materials. Parent/child determinations in cubic materials must rely on other EBSD-based statistical measures that will be discussed later.

Pre-program

As with the previous method (Henrie *et al.*, 2005) we use the OIM™ Analysis software to group scan points together into grain fragments and whole grains, and assign identification numbers to each. This is done for both fragments and whole grains using the built-in misorientation and twin boundary identification of OIM™ Analysis, both typically with a 5° tolerance. In identifying twin relationships, OIM™ Analysis allows the user to use any combination of the criteria defined by Mason *et al.* (2002) (misorientation axis/angle, K_1 matching, and alignment of the twin composition plane trace with the trace of a K_1 plane) to define twin boundaries. We use only the misorientation criterion, where fragment boundaries are classified as twin boundaries if the misorientation of any neighbouring scan points across the boundary is within the user-defined threshold. This involves using the misorientation analysis discussed above, and can be visualized as rotating the orientation of one fragment by the twinning relationship and measuring whether the two fragment orientations are then coincidental to within the misorientation tolerance.

We have found there is no benefit in using a K_1 matching criterion in addition to a misorientation criterion. K_1 matching can be visualized as rotating the orientation of one fragment by the twinning relationship and measuring whether the K_1 normal directions for the two fragments are the same within some tolerance. Both a misorientation and K_1 matching criteria might be used if the deviations from the ideal twin misorientation are concentrated about the K_1 axis. Figure 2 is a Rodrigues plot showing the distribution of misorientations

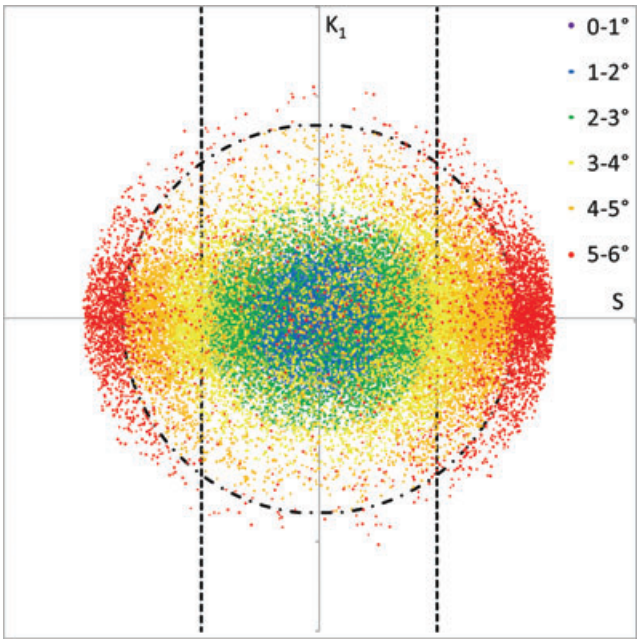

Fig. 2. Rodrigues space representation of the distribution of misorientations between M_{ab} and M_t (Eq. 5) for all fragments sharing a legitimate twin relationship measured in uranium. In Rodrigues space the direction of the Rodrigues vector represents the axis of misorientation, and the magnitude of the Rodrigues vector is proportional to the angle of misorientation, with two fragments sharing an exact twin relationship represented by a point at the origin. This figure is a projection of Rodrigues space along η_1 with S along the x-axis and K_1 along the y-axis and misorientation angles (radii) represented by colours. There is a misorientation angle cut-off of at 6° because of the tolerance used within the twin program to define twin boundaries. A slice of a 5° misorientation sphere and 3° K_1 matching tolerance hyperboloid (approximately vertical lines) are represented as dashed curves. This figure shows that there is no preference for the misorientation away from the exact twin misorientation relationship (0°) to be about the K_1 axis as has been assumed previously, but rather the S-axis.

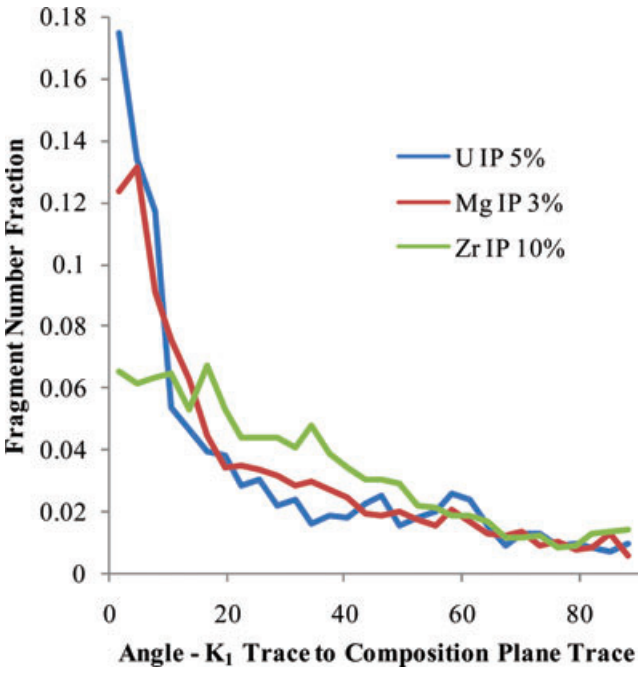

Fig. 3. Distribution of angles between K_1 traces and the major axes of ellipses fit to fragments, assumed to be parallel to the average composition plane trace, for Zr, Mg and U showing a large range of variation in angles between K_1 traces and twin composition planes.

between M_{ab} and M_t for all fragments sharing a legitimate twin relationship in an analysed uranium sample with figure details given within the caption. The conclusion from Fig. 2 is that there is no preference for the misorientation away from the exact twin misorientation relationship (0°) to be about the K_1 axis, but rather about the *S*-axis. Zr and Mg exhibit more uniform misorientation distributions than *U*, but none exhibit a preference for misorientations aligned about K_1. In light of these experimental results, it appears that nothing is gained by using a K_1 matching criterion in addition to a misorientation criterion.

We do not use the composition plane alignment with the trace of the K_1 plane criterion because it is too stringent for more heavily deformed materials where twins can deviate considerably from coherency as has been suggested previously (Mason *et al.*, 2002; Wright *et al.*, 2002). Figure 3 shows for Zr, Mg and U the distribution of angles between K_1 traces and the major axes of ellipses fit to twins, the ellipses major axes assumed to be parallel to the average composition plane trace. Although this is not the exact method used for this criterion within OIM™ analysis, it does show that there is a large range of variation in angles between K_1 traces and composition plane traces.

Using the misorientation criteria, around 5% of all boundaries that should be classified as general grain boundaries are classified as twin boundaries resulting in two or more whole grains being combined. This mis-grouping of adjacent grains is a result of the statistical probability that some common grain boundaries will have a misorientation close to a characteristic twin boundary misorientation. There is one of these erroneous twin boundary relationships in Fig. 1 between one of the family 3 fragments and the neighbouring whole grain in the upper left of the figure (boundary coloured red) resulting in the two whole grains being initially grouped together. Although we could use the alignment between the trace of the twin composition plane and the trace of the K_1 plane as a check against these boundaries [9], this approach is not foolproof and usually results in actual twin boundaries not being classified as such. Our solution, at this point, is to manually generate a list of those fragments that should be split from whole grains and place them in a new whole grain. Additionally, the user can choose to add fragments to a pre-existing whole grain if some twin boundaries have not been recognized as such by the OIM™ analysis software. These two procedures are accomplished using OIM™ Analysis to visually find the obviously mischaracterized boundaries and then creating a file containing the fragment numbers to be split off into their own whole grains or added to pre-existing whole grains by the twin code. These two steps are necessary for correct identification of parent fragments within a whole grain. Any fragment wrongly placed in a whole grain or missing from it is likely to cause errors in the analysis of the entire whole grain.

Similar to the previous method (Henrie *et al.*, 2005), the grain fragment and whole grain data within OIM™ Analysis is exported as three text files to be used by the twin program. The first two files are nearly the same in that they both list data for every scan point, but the first file contains the fragment ID and the second the whole grain ID. These two files are used to determine the association between fragment and whole grain as well as to calculate the length of boundaries between neighbouring fragments and whole grains, a new and particularly useful feature of the program. The third file contains data for each fragment including the fragment ID, average orientation, average position, size (number of scan points), fitted ellipse dimensions and the number and IDs of all neighbouring grain fragments.

Although the majority of input data for the program comes from the three files exported by OIM™ Analysis, a few user-generated files are also necessary. These include the files specifying fragments belonging to whole grains that should be split into new whole grains and the fragments which should added to existing whole grains as discussed previously, as well as a file with information about the crystal system (Laue group, unit cell parameters and the twinning modes, twin types, K_1s and η_1s).

Twin program

The twin program can be broken down into several steps that will be described in the following sections. The first steps prepare the data for the automated twin identification by first

defining the relevant crystallographic parameters and then reading in the scan data. These steps are followed by steps that check the misorientations between fragments and group fragments into families, remove incorrect twin relationships, and determine the phase (parent, twin type and generation, or other) for each family.

Data preparation for analysis

One of the major improvements of the program, the ability of the program to analyse any type of twin in any crystal system, begins with the initial portion of the program where the Laue group, lattice constants and twin parameters are read. From these, the orthonormal representation of R^{tw} and the twin transformation matrix, t, for each twin system are established along with the crystal symmetry elements, L_i. This is different from previous versions of the code (Henrie *et al.*, 2005) where K_1 normal directions, η_1 directions and material specific misorientation angles were hardwired into the program for a handful of specific metals.

Another major improvement of the code is the determination of shared boundary lengths between neighbouring fragments, families and whole grains, and the positions of whole grain triple points. This information becomes invaluable in making parent/twin determinations and for handling circular twin relationships as will be shown shortly. The second portion of the program involves reading in the OIM$^{\mathrm{TM}}$ Analysis generated files and the files that either split fragments from or add them to whole grains. As with the previous code (Henrie *et al.*, 2005) this is done to assign a whole grain ID to each fragment. While reading these files we also calculate the shared boundary lengths between neighbouring fragments and find the positions of whole grain triple points. At this point, each fragment has associated with it a fragment number, a whole grain number, an average orientation, an average position, a size, fitted ellipse dimensions and neighbour fragments and their shared boundary lengths.

Misorientation checks

For each whole grain, each pair of fragments is checked to determine whether they share the same orientation, a twin relationship, or no special relationship. Two fragments are determined to have the same orientation if their misorientation, $L_i g_b g_a^T L_j^T$, is less than some tolerance angle (generally 15°) for any combination of symmetry operations. We use the misorientation between $L_i g_b g_a^T L_j^T$ and $R_{\mathrm{tw}}^T t R_{\mathrm{tw}}$ discussed above for each symmetry operation to determine whether two fragments share a twin relationship. For calculating a twin misorientation in the twin program we use a somewhat larger tolerance angle (6°–8°) because we are considering average fragment orientations instead of individual scan points across the boundary as considered by OIM$^{\mathrm{TM}}$ Analysis, and because we do not have to worry about the misclassification of boundaries between whole grains. This is also different from the previous code (Henrie *et al.*, 2005), where two fragments were determined to have a twin relationship if they fulfilled a K_1 normal matching criterion (the actual criterion used was whether the K_1 normal directions of the two fragments were diametrically opposed) and an η_1 matching criterion. The old criteria and our misorientation criterion give very similar results for the same tolerance angle, but the K_1/η_1 matching criteria are actually only correct for type II twins and compound twins. For type I twins, it would be appropriate to check that the K_1 directions matched and that the η_1 directions were diametrically opposed.

If a twin relationship is found between two fragments, Schmid factors are calculated for each of these fragments based on the macroscopic stress state of the sample. Although the local stress states within grains deviate somewhat from the macroscopic stress state because of grain interactions, and these deviations are likely important during twinning and other deformation processes, a Schmid factor based on the macroscopic stress state of the sample is a very good indicator of twinning probability (Caplungo *et al.*, 2009). A twin thickness is also calculated for each of these fragments as if it is the twin. At this point, the parent and child determination for the relationship has not been determined. Once the relationship is established, the thicknesses associated with twin fragments can be meaningfully used. The twin thickness, however, is not the thickness measured on the EBSD scan plane (ellipse minor axis) but is the width of the twin along the K_1 normal direction. Once K_1 is established by defining the twin relationship between two fragments, the corrected thickness is calculated by multiplying the ellipse minor axis with the cosine of the angle between the K_1 and the scan normal.

With relationships between all fragments within a whole grain determined, fragments sharing similar orientations within the whole grains are grouped into families. Figure 4(a) shows schematically the twin relationships between families in the whole grain in Fig. 1, where the different coloured arrows indicate the type of twin relationship observed between the families, the colours consistent with the boundary colour scheme in Fig. 1(b). At this point each family has associated with it a size, a boundary length and a relationship (twin or not) with every other family in the whole grain. For each twin relationship between two families there is a Schmid factor in each family and a shared boundary length. The size and total boundary length are determined by summing the size and shared boundary lengths of all fragments within the family. The twin relationship is determined by examining the twin relationships between all pairs of fragments within the two families. Usually, the fragment relations between two families are of the same type. In rare cases, such as when two twin types share a similar misorientation with the parent such as the case for $\{172\}$ and $\{112\}$ twin in U ($\sim$13° difference), the fragment relations between two families, especially in heavily

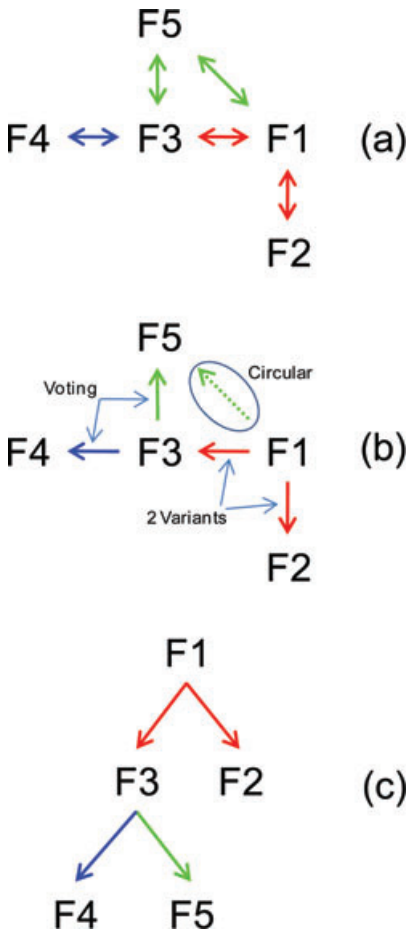

Fig. 4. Schematic representations of the whole grain in Fig. 1 showing (a) twin relationships between families, (b) removal of the errant circular relationship and parent/child identification between families sharing legitimate twin relationships and (c) formation of the twin family tree based on parent/child determinations.

deformed material, may not all be of the same twin type. In these rare cases, the program assigns only the twin type shared in the majority of fragment relations. The Schmid factor is the average Schmid factor for all fragment pairs sharing the twin relationship, and the shared boundary length is the sum of all shared fragment boundary lengths between the two families.

Voting schemes

As with the previous code (Henrie *et al.*, 2005), we implement voting schemes within our code to determine the parent family within each whole grain. However, we have added/modified some voting parameters, Schmid factor, size and boundary ratio, to improve the accuracy of the parent determination. For a large majority of twins, the Schmid factor (m) in the parent is positive and the Schmid factor in the twin is negative and the two are of similar magnitudes. Size (a), or majority rule, is a good determining factor of parent and twin for some materials (e.g. fcc materials) and low strain conditions. We have found a good morphology-based factor to be a comparison of boundary length ratios as a twin tends to share a larger percentage of its boundary with its parent than the percentage of boundary the parent shares with the twin. We define the boundary length ratio for family 1 with regard to family 2 as the boundary length shared between family 1and family 2 (b_{12}) divided by the total boundary length of family 1 (b_1).

For two families sharing a twin relationship, each family receives votes (V_1 for family 1 and V_2 for family 2) according to the following formulae with the family having the higher vote total considered the parent.

$$V_1 = S_f\,(m_1 - m_2) + A_f\left(\frac{a_1 - a_z}{a_1 - a_z}\right) + B_f\left(\frac{b_{1z}}{b_z} - \frac{b_{1z}}{b_1}\right) \quad (6)$$

$$V_2 = S_f\,(m_2 - m_1) + A_f\left(\frac{a_z - a_1}{a_1 - a_z}\right) + B_f\left(\frac{b_{1z}}{b_1} - \frac{b_{1z}}{b_z}\right) \quad (7)$$

The variables S_f, A_f and B_f are weighing factors for Schmid factor, area and boundary ratio votes, respectively, and can be used to weigh the voting parameters differently or to selectively turn on and off the different voting parameters. Figure 5 shows graphical representations of the voting parameters based on experimental data for several straining conditions for Zr, Mg and U (the legend entries indicate the material, straining direction, whether the straining direction is through thickness (TT) or in-plane (IP), and level of strain). These data are based on fragments having twin relationships in which the parent and child determinations have been manually confirmed. Figure 5(a) is a plot of $(b_{12}/b_2 - b_{12}/b_1)$ versus $(m_1 - m_2)$, where family 1 has been determined to be the parent and family 2 the child. For a voting scheme in which A_f is set to 0 and S_f, and B_f are both set to 1, everything below the line of slope 1 has a higher vote total. One thing this plot shows is that although most twins form on high Schmid factor twin systems, when they do form on lower Schmid factor twin systems, the difference between the twin boundary ratios tend to be high. Figure 5(b) is a plot of $(a_1 - a_2)/(a_1 + a_2)$ versus $(m_1 - m_2)$ again with family 1 being parent and family 2 the child. For a voting scheme in which B_f is set to 0 and S_f and A_f are each set to 1, everything below the line of slope minus 1 has a higher vote total. These two plots show that appropriate voting schemes can be very effective in making parent/child determinations.

Circular relations

Up to this point, all twin relationships between whole grain families are included based upon misorientation. However, this often includes some erroneous relationships arising from certain geometric conditions. These erroneous relationships result in a closed loop between three or four families, and make the determination of the parent very difficult. Therefore, we have added a step in the code to eliminate the invalid twin relationships. For Zr, there are

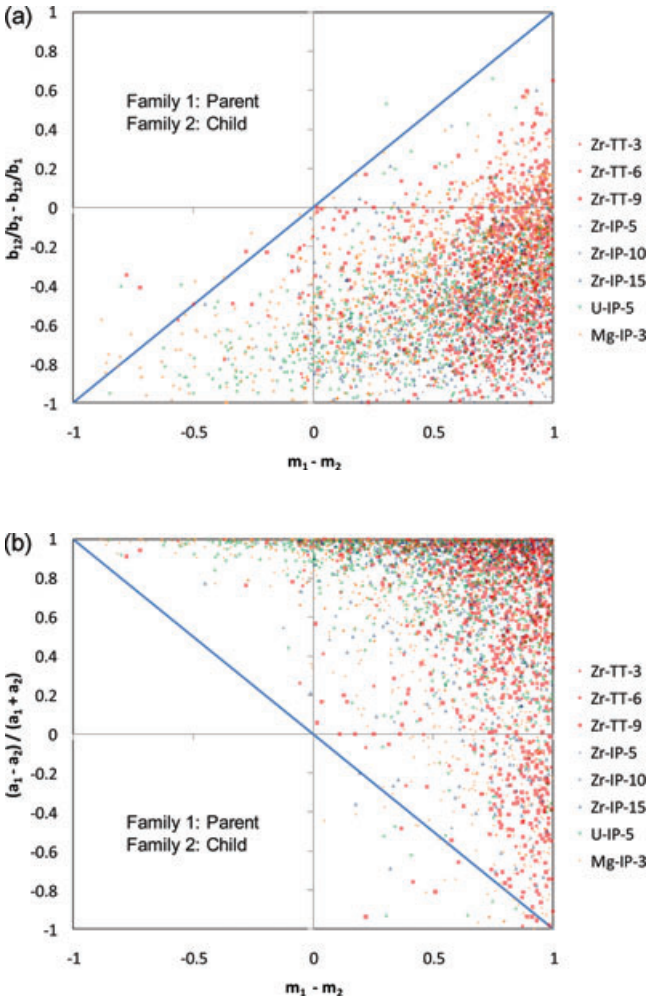

Fig. 5. (a) Experimental data for parent/twin boundary ratio difference versus parent/twin Schmid factor difference. A voting scheme correctly determines the parent and child using these two parameters for all data points below the blue line of slope 1 running through the origin. (b) Parent/twin size ratio difference versus Schmid factor difference for the same data. A voting scheme correctly determines the parent and child using these two parameters for all data points above the blue line of slope minus 1 running through the origin. Legend entries indicate the material, straining direction (TT or IP), and level of strain.

at least four geometric conditions resulting in circular twin relationships between three or four families. The easiest circular relationship to visualize occurs in the whole grain shown in Fig. 1(a) and is schematically represented in Fig. 4(b). Based on misorientation alone, family 1 has a $\{11\bar{2}2\} < 11\bar{2}3 >$ relationship (C1) with family 3, family 3 has a $\{11\bar{2}1\} < 11\bar{2}6 >$ relationship (T2) with family 6, and family 6 has an erroneous $\{11\bar{2}1\} < 11\bar{2}6 >$ (T2) relationship with family 1. Within our code we use the twinning transformation matrices, t, in Eq. 3 to define twin boundary misorientations because of its generality. However, there are other, equivalent misorientation matrices that can be used to define twin boundary misorientations that are more useful in understanding circular relations. The C1 misorientation for Zr can be defined as a 64.3° rotation about $< 10\bar{1}0 >$ and the T2 misorientaion can be defined as a 34.7° rotation about $< 10\bar{1}0 >$. For certain combinations of a second generation T2 twin within a first generation C1 twin, as occurs in Fig. 1, the parent and the second generation T2 twin also share a T2 misorientation relationship, although not an actual twin relationship, because a rotation of 64.3° about $< 10\bar{1}0 >$ minus a rotation of 34.7° about $< 10\bar{1}0 >$ is equivalent to a rotation of $34.7 \pm 5^\circ$ about $< 10\bar{1}0 >$.

The program removes one of the twin relationships when it finds any three or four family circular relationships as shown in Fig. 4(b). First, a voting scheme is used to determine the likely parent for each pair of families presenting a twin relationship. If, by this voting scheme, one of the families is determined to have two parents, one of the two relations with this family must be erroneous, and these two relations are further analysed as follows. The program compares the larger of the two boundary ratios (presumably that of the child) for the questionable twin relationships. If the smallest of these 'child' ratios is less than 90% of the second smallest, the twin relationship for the smallest is removed. Otherwise, a Schmid criterion is implemented where the questionable relationship with the smallest absolute Schmid factor is removed. In cases where none of the families have two apparent parents, all of the relations are further analysed using the method just described.

Pedigree

There are two steps involved in determining which family is parent between two families sharing a legitimate twin relationship. First, a family that has the same twin mode relationship with two or more other families (multiple variants) is considered the parent of all of those families. This stems from the assumption that a twin cannot have a child of the same twinning mode. This assumption is expected to be true for most materials undergoing monotonic deformation because of the dependence of twinning on the crystallographic orientation of the grain. The new orientation created during twinning is generally very unfavourable for the same type of twin to occur under the same stress-strain conditions. This assumption is probably not correct for complex changes in loading path (e.g. compression in the TT direction then the IP direction). In twin relationships where this does not apply, the program uses a voting scheme to compare the two families in question. Examples of both criteria are shown in Fig. 4(b).

We begin the assignment of twin generations at the top of the twin family tree. In a typical whole grain, there is one family that is the child of no other families. This family is declared the parent of the whole grain. All of the families that have legitimate twin relationship with the parent family are

categorized as first generation twins. The process of assigning children continues for unassigned families having a child relationship to a first generation twin. We continue the process for second generation, third generation, etc. twins until all of the families have been assigned, thus creating a twin family tree similar to the one shown in Fig. 4(c).

Manual corrections

After the twin family tree has been established for each whole grain in a scan, an OIM^{TM} Analysis readable file is output. The output file is similar to raw data EBSD files except that each scan point is assigned a phase designating whether the scan point is from a family designated as parent, a specific mode and generation of twin, or other (e.g. grain that did not twin). The result can be visually analysed with OIM^{TM} Analysis and corrections can be made for obviously mischaracterized whole grains. How often this occurs and the cause of the mischaracterizations are discussed in the following section.

Results and discussion

We describe here the performance of the twin program in determining the different twin modes and generations present in specific EBSD scans. Figure 6 shows orientation maps and twin maps for Zr, Mg and U. A twin map is an OIM^{TM} Analysis phase map created using the readable output file in which each phase represents parent material, a twinning mode and generation, or other. From these data, it is straightforward to determine area fractions and micro-textures for the different phases.

Table 1 shows some examples of twin statistics obtainable either directly with our program or using some of the additional output files. The statistics shown are far from exhaustive, and meant only to show some of the capabilities of the program, rather than a study of specific twinning mechanisms in a specific material. For more comprehensive application of the code to specific materials see references (Caplungo *et al.*, 2009; McCabe *et al.*, 2009).

Several observations can be made about the capability of the program based on the output shown in Table 1. Zr represents a challenge for any twin identification program, as it exhibits multiple twinning generations and three twinning modes with 18 total possible twin variants resulting in many possible circular relationships and other complexities. Zr also has considerable slip activity with slip accommodating 80–90% of the strain (McCabe *et al.*, 2009). This results in twin boundary misorientations that can vary considerably from the ideal twin misorientation relationship. These two factors are magnified with increasing strain. At the highest levels of strain reported here for Zr (IP13 and TT9), between 10 and 17% of the twinned whole grains had to be manually corrected following the initial running of the program. Around 40% of these corrections were because of the wrong relationship being removed from a circular relationship. Many of the others were because of the misorientation between parent and twin fragments being greater than the misorientation tolerance, in which case a twinning relationship had to be forced on the two representative families. Despite the complexities inherent with Zr, the new twin program is considerably more accurate than previous versions.

Mg represents a much easier test for the twin program because it primarily exhibits only one twinning mode, and slip only accommodates around half of the observed strain in the twinning regime of the stress strain curve. On average, no whole grains had to be manually adjusted in the Mg scans despite the fact that the twinned fraction was similar to that observed in the Zr at the highest strain levels. The success of the program on U is between Zr and Mg. U exhibits primarily three twinning modes with a total of 10 twin variants. U also exhibits considerable slip activity with roughly 75% of the strain accommodated by slip in the sample used in the current study.

Summary

EBSD data are well suited for studying deformation twinning because of its inherent spatially resolved orientation data. Taking advantage of EBSD data to extract twin statistics involves accurately determining which boundaries are twin boundaries (and of which type), and determining which of two grain fragments (or families) sharing a twin relationship is the parent and which is the child. We have developed a computer code to automatically perform these tasks and to extract other twin statistics using output files from OIM^{TM} Analysis. The primary benefits of our code compared to previous efforts include: handling materials of any crystal symmetry, handling a general stress state, improved accuracy and generating improved and additional statistics.

For defining twin boundaries we have shown there is no benefit to using a K_1 matching criterion in addition to defining twin boundaries based on misorientation. Similarly we have shown the criterion of matching the twin composition plane trace to the K_1 trace is too stringent for the materials studied.

Our analysis starts by having the OIM^{TM} Analysis software group neighbouring EBSD scan points into grain fragments and grain fragments into whole grains (grains in which twin boundaries are ignored). Data files based on these groupings are read into our twin program. The program then groups fragments within whole grains into families, makes parent/child determinations for families sharing twin relationships, determines the phase (twin mode and generation) and twin variant for each family based on all of the parent/child determinations for the whole grain, and then calculates other twin statistics. Various output files are generated including an OIM^{TM} Analysis readable file used for visualization where each twin mode and generation is defined as a phase, and several text files containing twin statistics.

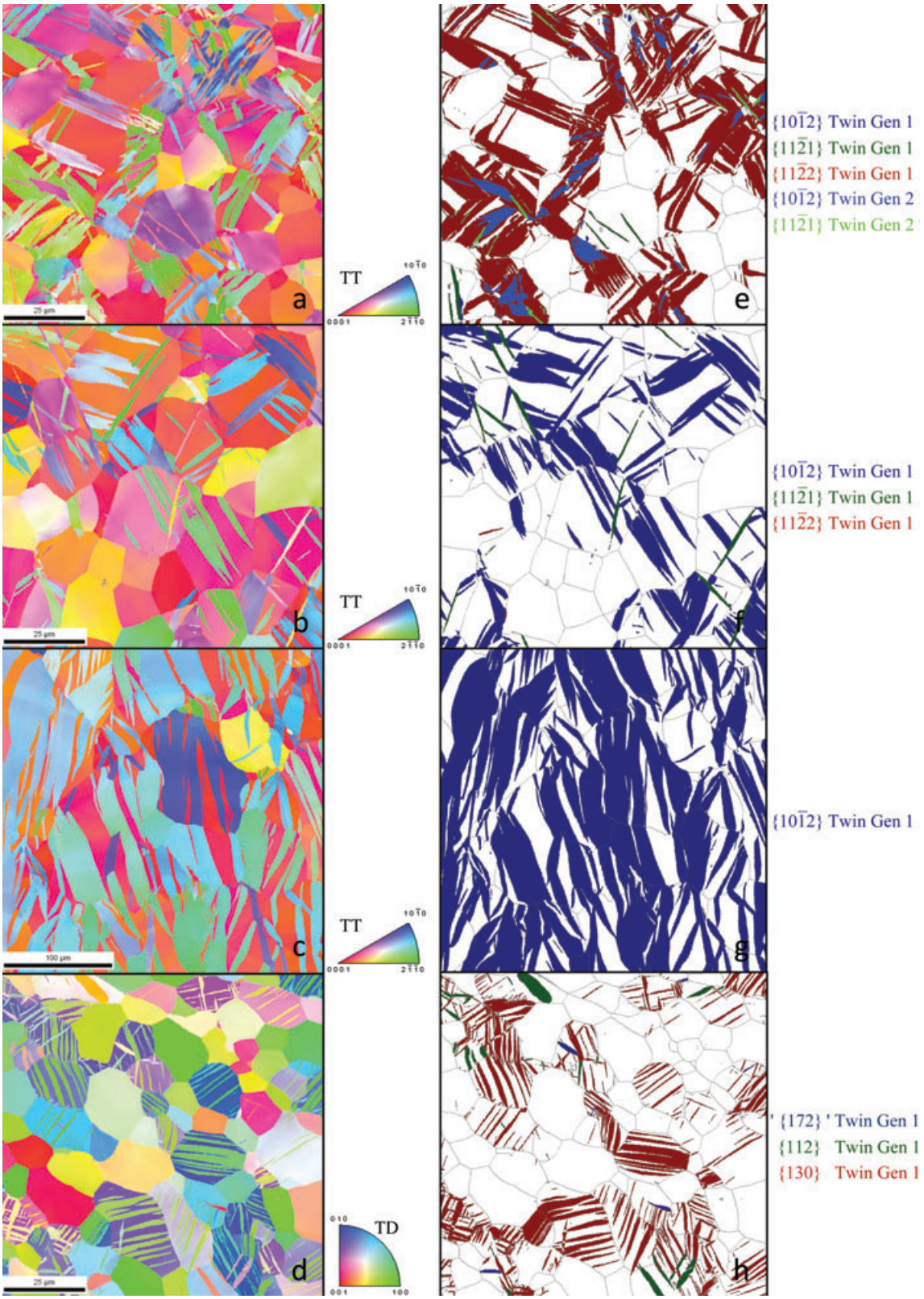

Fig. 6. Orientation maps and twin maps for (a) Zr compressed 6% in TT direction, (b) Zr compressed 9% in IP direction, (c) Mg compressed 3% in IP direction and (d) U compressed 5% in transverse direction direction. TT direction crystal orientations are shown for Zr and Mg, and the transverse direction direction crystal orientation is shown for U.

Table 1. Twin statistics obtained using our analysis code for different Zr, Mg and U specimens.

Material / strain	Number (#) of scans	Scan size mm^2	1st gen twin fract.	2nd gen twin fract.	Ave. twin thick. um	# of frags. per scan	# of twinned whole grains	# of manually corrected whole grains	# of split off whole grains	% circular twin relations
Zr-IP5	4	0.0288	0.056		0.262	562	85	0	9	6
Zr-IP9	7	0.0288	0.191		0.35	1333	124	1	18	12
Zr – I P13	1	0.0288	0.325	0.002		2222	158	27	20	13
Zr-TT3	1	0.0288	0.092		0.355	653	85	1	30	1
Zr-TT6	1	0.0288	0.329	0.025		1953	104	10	30	8
Zr-TT9	1	0.0288	0.465	0.074		3465	217	23	35	14
Mg-IP3	10	0.24	0.358		1.687	795	93	0	2	0
U-IP5	12	0.02	0.122		0.167	1937	57	1	4	9

We have applied our code to deformed microstructures of Mg, Zr and U. The program performed nearly flawlessly for the Mg and U microstructures studies and considerably better than previous programs for the complex deformation microstructures exhibited in Zr as can be seen from the twin maps and statistics obtained for the three materials.

Acknowledgements

We thank Benjamin Henrie for sharing his twin recognition code used as a starting point to this project. We also thank Ann Kelly for her metallographic expertise, Manny Lovato and Carl Cady for mechanical testing, Carlos Tomé for several discussions on the crystallographic implications of this work, and Stuart Wright at TSL/EDAX. The microscopy was performed at the Electron Microscopy Laboratory user facility at Los Alamos National Laboratory. This work was supported by funding from the Department of Energy, Office of Basic Energy Sciences Program FWP 06SCPE401, under U.S. DOE Contract No. W-7405-ENG-36.

References

Battaini, M., Pereloma, E.V. & Davies, C.H.J. (2007) Orientation effect on mechanical properties of commercially pure titanium at room temperature. *Metall. Mater. Trans. A* **38A**, 276–285.

Bingert, J.F., Mason, T.A., Kaschner, G.C., Maudlin, P.J. & Gray, G.T. (2002) Deformation twinning in polycrystalline Zr: insights from electron backscattered diffraction characterization. *Metall. Mater. Trans. A* **33**, 955–963.

Brown, D.W., Bourke, M.A.M., Clausen, B., Korzekwa, D., Korzekwa, R., McCabe, R.J., Sisneros, T.A. & Teter, D.F. (2009) Temperature and direction dependence of internal strain and texture evolution during deformation of uranium. *Mater. Sci. Eng., A* **512**, 67–75.

Caplungo, L., Marshall, P.E., McCabe, R.J., Beyerlein, I.J. & Tome, C.N. (2009) Nucleation and growth of twins in Zr: a statistical study. *Acta Mater.*, doi:10.1016/j.actamat.2009.08.030.

Courtney, T.H. (1990) *Mechanical Behavior of Materials*, McGraw-Hill, New York.

Glavicic, M.G., Salem, A.A. & Semiatin, S.L. (2004) X-ray line-broadening analysis of deformation mechanisms during rolling of commercial-purity titanium. *Acta Mater.* **52**, 647–655.

Henrie, B.L., Mason, T.A. & Hansen, B.L. (2004) A semiautomated electron backscatter diffraction technique for extracting reliable twin statistics. *Metall. Mater. Trans. A* **35A**, 3745–3751.

Henrie, B.L., Mason, T.A. & Bingert, J.F. (2005) Automated twin identification technique for use with electron backscatter diffraction. *Mater. Sci. Forum* **495–497**, 191–196.

Kalidindi, S.R. (1998) Incorporation of deformation twinning in crystal plasticity models. *J. Mech. Phys. Solids.* **46**, 267–290.

Kocks, U.F., Tome, C.N. & Wenk, H.R. (1998) *Texture and Anisotropy – Preferred Orientations in Polycrystals and their Effect on Materials Properties*. Cambridge University Press, Cambridge.

Livescu, V., Cady, C.M., Cerreta, E.K., Henrie, B.L. & Gray, G.T. (2006) The high strain rate deformation behavior of high purity magnesium and AZ31B magnesium alloy. *Symposium on Magnesium Technology 2006*. Minerals, Metals & Materials Soc., San Antonio, Texas.

Mason, T.A., Bingert, J.F., Kaschner, G.C., Wright, S.I. & Larsen, R.J. (2002) Advances in deformation twin characterization using electron backscattered diffraction data. *Metall. Mater. Trans. A* **33**, 949–954.

McCabe, R.J., Cerreta, E.K., Misra, A., Kaschner, G.C. & Tome, C.N. (2006) Effects of texture, temperature, and strain on the deformation modes of zirconium. *Philos. Mag. A* **86**, 3595–3611.

McCabe, R.J., Proust, G., Cerreta, E.K. & Misra, A. (2009) Quantitative analysis of deformation twinning in zirconium. *Int. J. Plast.* **25**, 454–472.

Proust, G., Tome, C.N. & Kaschner, G.C. (2007) Modeling texture, twinning and hardening evolution during deformation of hexagonal materials. *Acta Mater.* **55**, 2137–2148.

Randle, V. & Engler, O. (2000) *Introduction to Texture Analysis – Macrotexture, Microtexture, and Orientation Mapping*, Gordon and Breach Scientific Publishers, Amsterdam.

Salem, A.A., Kalidindi, S.R. & Doherty, R.D. (2002) Strain hardening regimes and microstructure evolution during large strain compression of high purity titanium. *Scripta Mater.* **46**, 419–423.

Tome, C.N., Lebensohn, R.A. & Kocks, U.F. (1991) Model for texture development dominated by deformation twinning. Application to zirconium alloys. *Acta Metall. Mater.* **39**, 2667–2680.

Van Houtte, P. (1978) Simulation of the rolling and shear texture of brass by the Taylor theory adapted for mechanical twinning. *Acta Metall* **26**, 591–604.

Wagoner, R.H., Lou, X.Y., Li, M., Boger, R.K. & Agnew, S.R. (2007) Hardening evolution of AZ31B Mg sheet. *Int. J. Plast.* **23**, 44–86.

Wright, S.I., Bingert, J., Mason, T.A. & Larsen, R.J. (2002) Advanced characterization of twins using automated electron backscatter diffraction. *Mater. Sci. Forum* **408–412**, 511–516.

Wu, X., Kalidindi, S.R., Necker, C. & Salem, A.A. (2007) Prediction of crystallographic texture evolution and anisotropic stress-strain curves during large plastic strains in high purity alpha-titanium using a Taylor-type crystal plasticity model. *Acta Mater.* **55**, 423–432.

Young, C.T. & Lytton, J.L. (1972) Computer generation and identification of Kikuchi projections. *J. Appl. Phys.* **43**, 1408–1417.

